A novel hybrid islanding detection method for inverter-based distributed generation based on frequency drift*

S Akhlaghi†
Department of Electrical Engineering, Islamshahr Branch, Islamic Azad University, Islamshahr, Iran

H Meshginkelk
Department of Electrical Engineering, University of Tafresh, Tafresh, Iran

A Akhlaghi
Department of Electrical Engineering, Islamshahr Branch, Islamic Azad University, Islamshahr, Iran

AA Ghadimi
Department of Electrical Engineering, University of Arak, Arak, Iran

ABSTRACT: *This paper proposes a novel hybrid islanding detection method for inverter-based distributed generation (DG) based on frequency drift. This algorithm is a combination of Sandia frequency-shift, reactive power versus frequency and reactive power deviation as active methods, and over/under frequency protection as a passive method. The performance of the proposed method is evaluated under the UL 1741 anti-islanding tests configuration, IEEE 1547, load switching, load quality factor and multiple-DG operation. The simulation results are derived by MATLAB/Simulink. Based on simulation results, it is clear that the proposed method is developed to detect islanding more efficiently for loads with high quality factor. The proposed method also has less non-detection zone comparing other methods. In addition, the proposed method operates accurately in condition of load switching while does not interfere with the power system operation during normal conditions. This technique proves to be robust under multiple-DG operation.*

KEYWORDS: Distributed generation (DG); inverter; islanding detection; non-detection zone (NDZ); Sandia frequency shift (SFS).

REFERENCE: Akhlaghi, S., Meshginkelk, H., Akhlaghi, A. & Ghadimi, A. A. 2014, "A novel hybrid islanding detection method for inverter-based distributed generation based on frequency drift", *Australian Journal of Electrical & Electronics Engineering*, Vol. 11, No. 2, June, pp. 161-174, http://dx.doi.org/10.7158/E13-085.2014.11.2.

NOMENCLATURE

Q-f	reactive power versus frequency
Q_{df}	reactive power deviation
R_g, L_g	resistance and inductance of power system line
R, L, C	load resistance, inductance and capacitance
L_{filter}	inductance of the inverter filter
k_P, k_I	proportional and integral control factors
θ_{SMS}	phase angle for slide-mode frequency shift method
θ_m	maximum phase angle in degree
f	frequency
f_g	grid frequency
f_m	frequency at which θ_m occurs
f_{is}	islanding frequency
Q_f	quality factor

* Paper E13-085 submitted 17/05/13; accepted for publication after review and revision 23/09/13.

† Corresponding author Shahrokh Akhlaghi can be contacted at shahrokh.akhlaghi@gmail.com.

I_d, I_q	*d-q* components of the current
v_d, v_q	*d-q* components of the point of common coupling voltage
I_{dref}, I_{qref}	reference current of *d-q* components
V_{dref}, V_{qref}	reference voltage of *d-q* components
M	modulation index amplitude
φ	phase angle

1 INTRODUCTION

It is an undeniable fact that usage of distributed generation (DG) resource are growing rapidly. In the context of distributed energy resource units, an island is formed when a portion of the utility system that contains both load and DG resources remains energised while isolated from the rest of utility system (IEEE, 2003; Underwriters Laboratories, Inc., 2001). This process is called an islanding phenomenon and can occur due to pre-planned or intentional and accidental or unintentional events. The accidental or unintentional islanding of DG which can occur due to faults could cause negative impacts on distribution systems such as power-quality problems, equipment damage and even it can be dangerous to utility workers, who may not realise that a circuit is still powered. Also it may prevent interference of grid protection devices and automatic re-connection. Therefore, islanding must be rapidly detected within acceptable durations and then the circuit breaker between the power system and the DG should be immediately tripped, this is referred to as anti-islanding (Zeineldin, 2009). As highlighted in the IEEE Std 1547-2003 and IEEE Std 929-2000, unintentional islanded DG systems require to be shut down within a predefined time period. Hence, one of the most technical challenges associated with DG operation is islanding detection.

The main philosophy of detecting an islanding situation is monitoring the DG output parameters and system parameters such as voltage amplitude, phase difference and frequency variation and then deciding whether or not an islanding situation has occurred due to changing in these parameters. Islanding detection techniques can broadly be divided into remote and local techniques. Remote islanding detection techniques are based on communication between utilities and DGs. These techniques may provide more reliability than local techniques; however, they are expensive to implement and hence uneconomical. On the other hand, since local techniques are based on the information on the DG site, it would be predictable that these techniques are not as expensive as remote techniques. Based on these reasons, local techniques have been recently used in most of the researches of islanding detection and can further be divided into active, passive and hybrid detection techniques, which can be specific for synchronous generators, inverter-based DG resources or both units as shown in figure 1.

Passive methods measure voltage amplitude, frequency change, harmonic distortion and phase displacement information at the point of common coupling (PCC). Differentiation between an islanding and grid connected condition is based upon the thresholds set for these parameters. Special care should be taken while setting the threshold values so as to differentiate islanding from other disturbances in the system (Zeineldin & Kirtley, 2009a; 2009b).

The over/under voltage protection (OVP/UVP) and over/under frequency protection (OFP/UFP) (Zeineldin & Kirtley, 2009a; 2009b) are conventional relays of islanding detection which are able to detect an islanding condition by considering the difference between the voltage and the frequency of voltage at PCC and comparing them with pre-set threshold, whereas phase jump detection monitor the phase difference between the voltage of DG terminal and its output current to trigger the protection circuit (Singam & Huil, 2006). Rate of change of active power (De Mango et al, 2006; Zhou et al, 2013) that is symbolised with dp/dt, tends to increase significantly in dp/dt in the event of islanding causing tripping relay to operate. On a similar basis, rate of change of frequency (ROCOF) (Freitas et al, 2005) relay monitors the df/dt of the power system and if this parameter goes beyond of trip setting period, islanding condition will be detected. On the other hand, for less sensitivity to sudden change of load during normal operating condition and higher responsiveness of islanding detection, ROCOF over power (Zhou et al, 2013) is introduced that is denoted by df/dp.

Other main passive islanding detection methods (IDMs) are voltage amplitude (Freitas et al, 2005), voltage and power factor changes (Huang & Pai, 2000), system impedance (Kim & Hwang, 2000), voltage imbalance and total harmonic distortion (THD) (Liu & Thomas, 2011; Massoud et al, 2009). These parameters are compared with pre-set thresholds to detect an islanding condition. While vector surge relay, OFP/UFP and ROCOF are very commonly used in synchronous DGs and harmonic distortion methods such as voltage and current harmonic detection methods are very suitable for inverter base DGs, other methods are classified as general techniques (Massoud et al, 2009). Passive techniques are fast and they don't introduce disturbance in the system but they have a large non-detection zone (NDZ) where they fail to detect the islanding condition (Zeineldin, 2009). The main issue in passive methods refers to suitable choice of appropriate thresholds such that the anti-islanding relays have highest reliability. For inverter based DG, flexible operation is possible with passive methods.

Active detection methods are known as an alternative for passive methods. In this case, to minimise or avoid NDZ, a deliberate disturbance is injected at system voltage, frequency or phase angle. This small

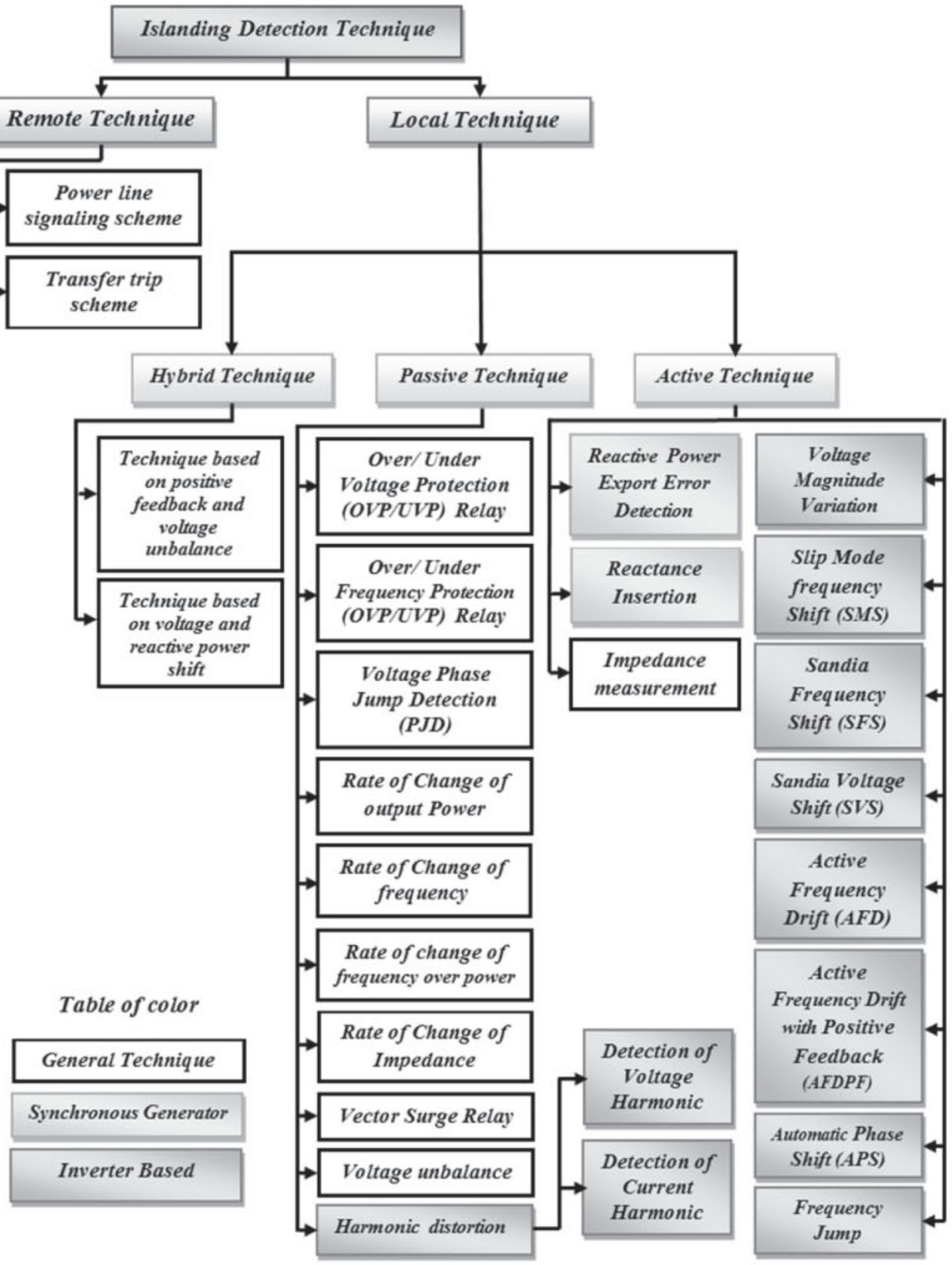

Figure 1: Islanding detection techniques.

perturbation will result in a significant change in system parameters such as amplitude and frequency of the output voltage, output current, output power or relative phase angle of the DG output when the DG is islanded and cause to operate existing relays on distribution system.

Active methods include Sandia voltage shift (SVS) (Freitas et al, 2005), Sandia frequency shift (SFS) (Zeineldin & Kennedy, 2009a; Zeineldin & Salama, 2011; Vahedi & Karrari, 2013; Lopes & Sun, 2006; Chang, 2013; Vahedi et al, 2011) and slide-mode frequency shift (SMS) (Kamyab & Sadeh, 2013) that apply positive feedback to the amplitude, frequency and phase of the PCC voltage, respectively (Lopes & Sun, 2006). On the other hand, active frequency drift (AFD) or frequency bias technique drifts the frequency of the voltage (at the PCC in the island) up or down. This is mainly to surpass present tripping level for inverter to shut down when islanding occurs, whereas SFS performs the same detection approach as AFD but with additional positive feedback to reinforce larger frequency errors (Chang, 2013). For SVS scheme, in the islanding situation, the voltage at the PCC is reduced followed by the reduction of inverter output power and output current (Freitas et al, 2005). Automatic phase shift method repairs the non-detection problems of SMS and AFD methods by injecting additional phase shift whenever the frequency of the terminal voltage reaches steady-state (Wang et al, 2007).

Some approaches such as reactive power export error detection, fault level monitoring, under/over voltage protection relays, OVP/UVP relays, ROCOF, phase displacement monitor relays and SFS have

already been commercialised, while other methods are currently under investigation. Up to now, many anti-islanding approaches have been proposed in the literature (Freitas et al, 2005; Ropp & Bower, 2002); but to find a low cost, quick and reliable method is still known as an open problem.

Most of previous studies used SFS method for islanding detection of inverter base DG since it is easy to implement. However, the constant power controlled inverter that is equipped with the SFS IDM performs poorly for islanding detection. *Q-f* droop curve method forces the DG lose its stable operation once an islanding condition occurs. Although, these methods take a lot of time to detect islanding, and also they are not able to detect islanding for loads with high quality factor.

In this paper, an effective hybrid IDM including passive and active parts is proposed. The proposed islanding detection strategy takes advantages of both active and passive IDMs. This proposed method is a combination of SFS, reactive power versus frequency (*Q-f*), reactive power deviation (RPD) as active methods and OFP/UFP as passive method. The major novelty of the proposed technique is firstly compensating the deficiency of the SFS method which is poor performance in islanding detection of inverter controlled with constant power. Secondly, this hybrid method is more efficient than its components, since it is able to detect islanding for inverter- based DGs in less duration of time for loads with high quality factor. The proposed method also is capable of riding through disturbances such as load switching. In addition, the performance of the proposed islanding detection technique is tested under different loading conditions such as UL 1741 anti-islanding tests configuration, IEEE 1547, load quality factor, load switching and multiple-DG operation.

The paper is organised as follows. Section 2 presents the system and DG interface model under study. Section 3 presents the proposed islanding detection technique. The NDZ of proposed method is presented in section 4. Section 5 presents the performance of the proposed islanding detection technique. Lastly, conclusions are drawn in section 6.

2 DG SYSTEM AND INTERFACE MODEL

The performance of the proposed islanding detection technique is tested on the system shown in figure 2. This system consists of a distribution network displayed by a source behind impedance, a load displayed in terms of R-L-C and a 100 kW inverter-based DG. The inverter, grid, load and DG controller parameters are listed in table 1.

2.1 DG interface controller models

The DG was implemented and designed to operate as a constant power source by adjusting the

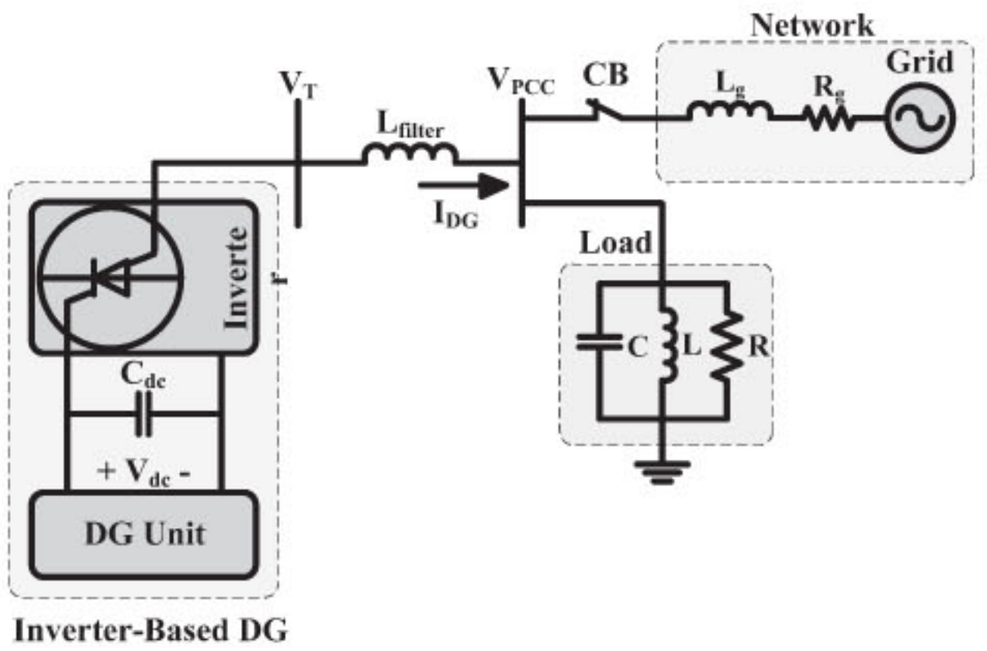

Figure 2: System under study.

Table 1: Inverter, system, load and DG parameters.

Inverter parameters		
Switching frequency	8000 Hz	
Input DC voltage	900 V	
Filter inductance	2.1 mH	
Voltage (line to line)	480 V	
DG output active power	100 kW	
Grid parameters		
Frequency	60 Hz	
Grid inductance	0.3056 mH	
Grid resistance	0.012 Ω	
Load parameters		
Resistance	2.304 W	
Inductance	0.00345 mH	
Capacitance	2037 μF	
Constant power controlled inverter parameters		
Power regulator	$k_P = 0.025$	$k_I = 7$
Current regulator	$k_p = 0.85$	$k_I = 8$

controller's active and reactive reference values to fixed prespecified values with no grid supporting capability (Underwriters Laboratories, Inc., 2001). The *d-q* synchronous reference frame is used to control the DG interface control variables. Equations (1) and (2) represent the instantaneous real and reactive power in terms of the *d-q* axis components as follows:

$$P = \frac{3}{2} v_{td} i_{td} \tag{1}$$

$$Q = \frac{3}{2} v_{tq} i_{tq} \tag{2}$$

The *a-b-c* three-phase DG output currents are measured and transformed using Park's transformation into its *d-q* components (i_{td} and i_{tq}) and v_{td} and v_{tq} represent the *d-q* components of the PCC voltage.

As can be seen in figure 3, to generate i_{dref} and i_{qref}, active and reactive powers reference values and reactive power deviation (Q_{df}) are compared with the measured DG active and reactive powers output then pass through a power regulator. Then, I^*_{dref} and I^*_{qref} are obtained by applying a phase angle transformation defined in equation (3).

$$\begin{bmatrix} I^*_{dref} \\ I^*_{qref} \end{bmatrix} = \begin{bmatrix} \cos\theta_f & -\sin\theta_f \\ \sin\theta_f & \cos\theta_f \end{bmatrix} \begin{bmatrix} I_{dref} \\ I_{qref} \end{bmatrix} \quad (3)$$

Next, I^*_{dref} and I^*_{qref} are compared with i_d and i_q which are the inverter output currents. Then, pass through current regulator to the outputs V_{dref} and V_{qref}. Given equation (4), V_{dref} and V_{qref} transform to V_{sd} and V_{sq}.

$$\begin{aligned} V_{sd} &= V_{dref} + V_{td} - L_f \omega I_q \\ V_{sq} &= V_{qref} + V_{tq} - L_f \omega I_d \end{aligned} \quad (4)$$

where V_{td} and V_{tq} represents the *d-q* components of the PCC voltage and L_f is the filter inductance. The outputs of the current regulators V_{sd} and V_{sq} are the inverter terminal voltages. These components are used to calculate the modulation index amplitude (M) and phase angle (φ) which are calculated from equations (5) and (6). Sinusoidal pulse-width modulation is implemented to determine the on and off signals of the inverter switches. This type of interface is capable of controlling the DG active and reactive power output.

$$M = \sqrt{V^2_{dref} + V^2_{qref}} \quad (5)$$

$$\varphi = \tan^{-1} \frac{V_{qref}}{V_{dref}} \quad (6)$$

3 PROPOSED ISLANDING DETECTION TECHNIQUE

The proposed method in this paper is a novel hybrid method for detect the islanding phenomena that is based on drift the frequency of the voltage at the PCC. The propose method to detect an islanding situation needs to a simple passive islanding detection scheme based on frequency relay such as OFP/UFP. This proposed method is a combination of Sandia frequency-shift (SFS), reactive power versus frequency (*Q-f*), RPD, whichever are not for efficiently and accurately detecting islanding for loads with high quality factor. The suggested method is combined with inverter control system as shown in figure 3 and its components will explain as follows.

3.1 SFS model

The SFS scheme is a positive feedback anti-islanding method that uses the deviation of frequency from normal value as the feedback signal to influence the operation of the inverter (Lopes & Sun, 2006). The inverter output current using this method is given by:

$$i_k = \sqrt{2} I \sin\left[2\pi f_{(vk-1)} t + \theta_{SFS}\right] \quad (7)$$

The angle θ_{inv} used in the transformation block is determined from the SFS control block which is shown in figure 3. For the SFS IDM, the feedback signal (θ_{inv}) can be expressed as a function of the PCC voltage frequency (f), grid frequency (f_g), positive feedback gain (k) and initial chopping fraction (Cf_o) which is obtained through equation (8) (Zeineldin & Kennedy, 2009b).

$$\theta_{SFS} = \frac{\pi}{2}\left[Cf_\circ + k(f - f_g)\right] \quad (8)$$

The interactions between the constant power control of interface controls strategy of inverter-based DG and the SFS IDM are compared through electromagnetic transient simulations. In figure 4, the frequency of the voltage at the PCC before and after occurrence of an islanding event for the constant-power controlled inverter in four scenarios are presented. In the simulations, IEEE 1547-2003 recommends the operation of the DG close to unity power factor that is accomplished by setting Q_{ref} to zero and ΔP is zero for both the types of controllers

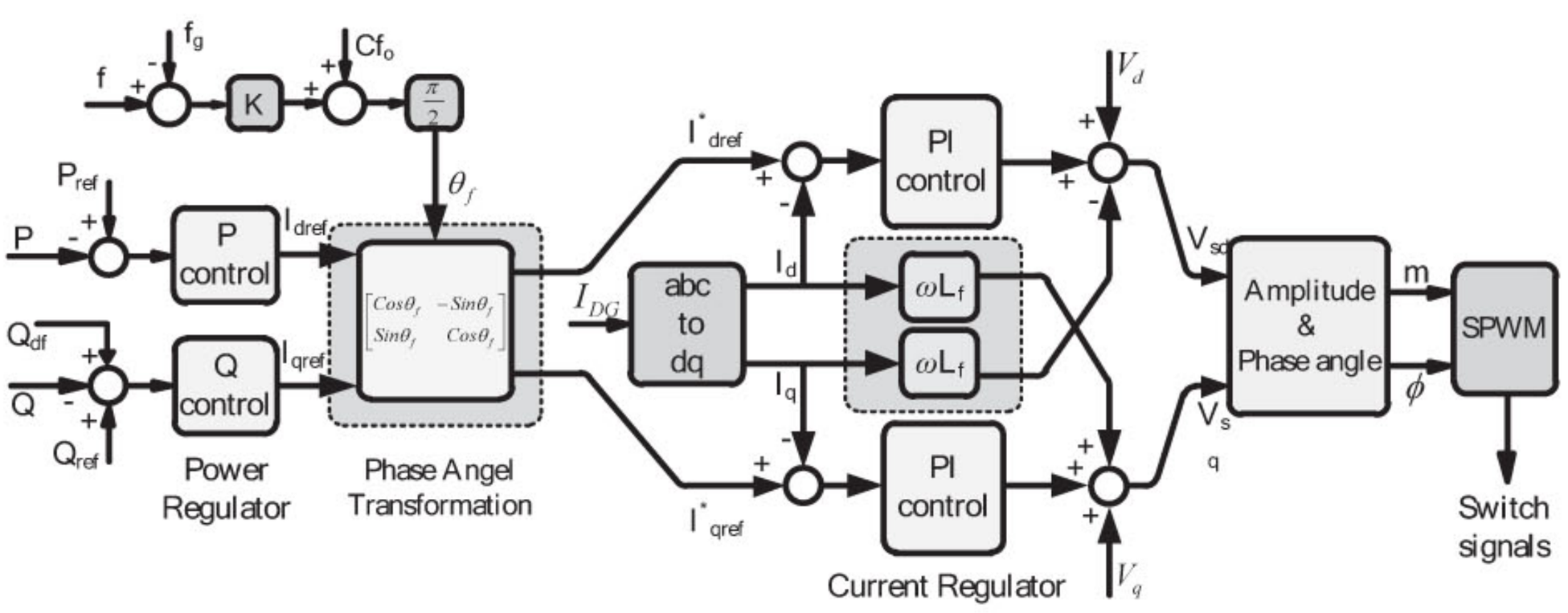

Figure 3: DG interface control for constant power controlled equipped with proposed methods.

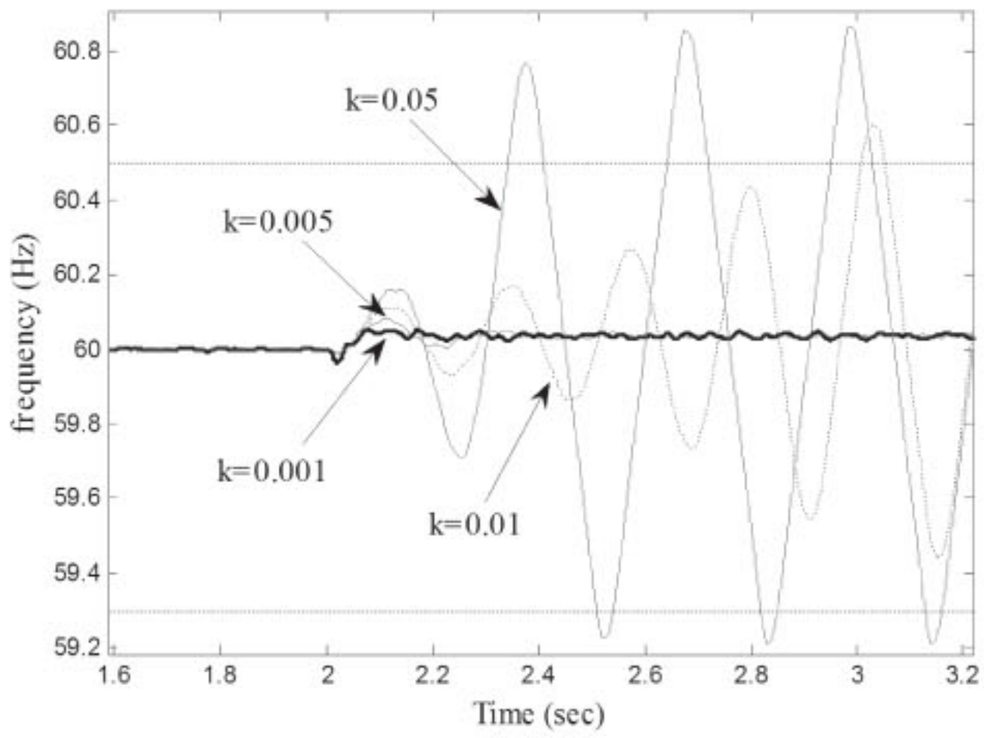

Figure 4: PCC voltage frequency with the SFS IDM for different *k*.

(IEEE, 2003). As a result, the load active power is only supplied by the DG; the resonant frequency of the R-L-C load is set as 60 Hz; the load quality factor is 1.77; Cf_o is adjusted in 0.03 so the THD of the inverter current is less than 5% at the rated line frequency; and the islanding occurs at the t = 2 s. In figure 4, when k is adjusted in 0.001 and 0.005, it can be seen that for these scenarios, the frequency of islanded DG system converges to a steady-state operating point for both values. The inverter steady-state frequencies after the islanding are 60.05 Hz for both cases. The later frequency is the steady-state frequency forecasted by the positive feedback gain of the SFS scheme, but the previous one is the resonant frequency of the R-L-C load. In third case k is increased to 0.01. The inverter frequency begins to fluctuate after the islanding. These cases illustrate that the SFS anti-islanding method does not work for the constant-power controlled inverter when the positive feedback gain (k) is small. The reason is that the power regulator of the constant power controller counteracts the k. In last scenario, k is further increased to 0.05, and the DG system is destabilised. For the constant power-controlled inverter, the strength of the power-control state cannot hit that of the SFS scheme when the main grid is disconnected. The inverter frequency begins to oscillate after the islanding, and the DG will be tripped by the frequency relay ultimately. However, it is to note that the islanding detection takes longer to be. It was found that the power regulator of the constant power controlled inverter can degrade the positive feedback control (Wang et al, 2007). Therefore, one can conclude that the SFS IDM is not suitable for constant power controlled inverter.

3.1.1 Non-detection zone of SFS method

Active and reactive power balances occur in the steady-state for a system with both sources and loads after it is disconnected from the grid. The reactive power balance condition can be defined using the load current angle (θ_{load}) and the inverter current angle (θ_{inv}). Thus, the steady-state value of the frequency of an islanded system (f_{is}) can be calculated using the phase criteria $\theta_{load} = \theta_{inv}$.

The current phase angle of a parallel R-L-C load as a function of the frequency is defined as:

$$\begin{aligned}\theta_{load} &= \arg\left\{R^{-1} + (j\omega L)^{-1} + j\omega C\right\}^{-1} \\ &= \tan^{-1}\left(R\frac{1-\omega^2 LC}{\omega L}\right) = \tan^{-1}\left[Q_f\left(\frac{f_o}{f} - \frac{f}{f_o}\right)\right]\end{aligned} \tag{9}$$

where the quality factor (Q_f) is defined as 2π times the ratio of the maximum stored energy to the energy dissipated per cycle at a given frequency. For a parallel R-L-C load:

$$\left.\begin{aligned} Q_f &= \frac{\pi(CR^2I^2)}{\pi RI^2/\omega_o} = \omega_o RC = \frac{R}{\omega_0 L} \\ \omega_o &= 2\pi f_o = \frac{1}{\sqrt{LC}} \end{aligned}\right\} \Rightarrow Q_f = R\sqrt{\frac{C}{L}} \tag{10}$$

The NDZ of the SFS IDM in the Q_f versus f_o space is derived using the phase criteria $\theta_{load} = \theta_{inv}$ (Zeineldin & Kennedy, 2009b):

$$-\tan^{-1}\left[Q_f\left(\frac{f_g}{f_{is}} - \frac{f_{is}}{f_g}\right)\right] = \frac{\pi}{2}\left[Cf_o + k(f_{is} - f_g)\right] \tag{11}$$

Thus:

$$f_g^2 + \frac{f_{is}\tan(\theta_{SFS})}{Q_f} f_g - f_{is}^2 = 0 \tag{12}$$

From equation (12), it can be seen that the NDZ will depend on a great extent on the SFS method parameter (k) and load parameters (f_o and Q_f). The equilibrium point defined by the phase criterion in equation (13) must be an unstable equilibrium in order to ensure islanding detection and to eliminate the NDZ. In the latter case, the critical point defined by the phase criteria corresponds to an unstable equilibrium point. To eliminate the NDZ it is necessary to ensure that for all possible loading scenarios, the load and DG phase angle intersection point is an unstable operating point. This condition can be expressed as (Zeineldin & Kennedy, 2009b):

$$\frac{d\theta_{load}}{df} < \frac{d\theta_{inv}}{df} \tag{13}$$

Using the slope criteria presented in equation (13), the value of k in equation (8) can be chosen to guarantee that the frequency will drift outside of the NDZ.

$$\frac{d\theta_{inv}}{df} = \frac{\pi}{2}k \tag{14}$$

The slope of the load voltage-current phase dependency on frequency could be expressed as follows:

$$\frac{d\theta_{load}}{df} = \frac{Q_f\left(\frac{f_g}{f_{is}^{\ 2}} + \frac{1}{f_g}\right)}{1+Q_f^2\left(\frac{f_g}{f_{is}} - \frac{f_{is}}{f_g}\right)^2} \quad (15)$$

The proposed method slope θ_m should be set greater than the load phase angle slope expressed in equation (16), leading to the following condition for instability:

$$k_1 > \max \frac{2\left[Q_f\left(\frac{f_o}{f^2} + \frac{1}{f_o}\right)\right]}{\pi\left[1+Q_f^2\left(\frac{f_o}{f} - \frac{f}{f_o}\right)^2\right]} \quad (16)$$

Here, particle swarm optimisation (PSO) algorithm is used to determine the maximum value in equation (16). The main objective to maximise is:

$$objective = \max \frac{2\left[Q_f\left(\frac{f_o}{f^2} + \frac{1}{f_o}\right)\right]}{\pi\left[1+Q_f^2\left(\frac{f_o}{f} - \frac{f}{f_o}\right)^2\right]} \quad (17)$$

The main constraints of the optimisation problem are:

$$0 < Q_f < Q_{fmax} \quad (18)$$

$$f_{min} < f < f_{max} \quad (19)$$

where Q_{fmax} represents the highest expected load quality factor or the IEEE standard testing value. IEEE 929-2000 proposes the use of a $Q_f \leq 2.5$. The parameters f_{min} and f_{max} represent the UFP/OFP thresholds and are taken to be 59.3 and 60.5 Hz in this paper, respectively (Zeineldin & Kennedy, 2009b). Table 2 shows the results obtained from the PSO algorithm for different values of Q_{fmax}. Thus, to eliminate the NDZ for loads with $Q_f \leq Q_{fmax}$, the SFS method parameter (k) should follow the constraint provided in table 2.

To calculate the NDZ of the SFS IDM, in equation (12) the islanding frequency (f_{is}) is first adjusted to a threshold frequency (f_{min} = 59.3 Hz or f_{max} = 60.5 Hz). Then the value of Q_f is varied and finally a calculation is made of the resonant frequency of the load at the threshold of the NDZ (Zeineldin & Kennedy, 2009b).

The effect of k on the NDZ can be seen in the f_o-Q_f space as shown in figure 5(a). The set of curves for different values of k define a shield, within which islanding will not be detected. It can be seen that for k set to 0.05, all loads with a quality factor that is less than approximately 2.5 would be detected. This result corresponds with the results presented in table 2. Figure 5(b) shows the NDZ for different values of Cf_o. Increasing the value of Cf_o distorts the shield downward, which could either increase or decrease the NDZ, depending on the value of the load's resonant frequency, f_o. An important conclusion is that the NDZ can be effectively eliminated using only a single SFS parameter. Since an increase in Cf_o would lead to higher harmonic distortion, using k as the design parameter would be preferred (Zeineldin & Kennedy, 2009b).

Table 2: Thresholds on the SFS method parameters for different Q_f.

Q_{fmax}	Threshold on k
1.00	0.02138
1.80	0.03783
2.12	0.04547
3.00	0.06422
4.21	0.09005
5.00	0.10709
6.31	0.13473
7.00	0.15011
8.10	0.17318
9.00	0.19132

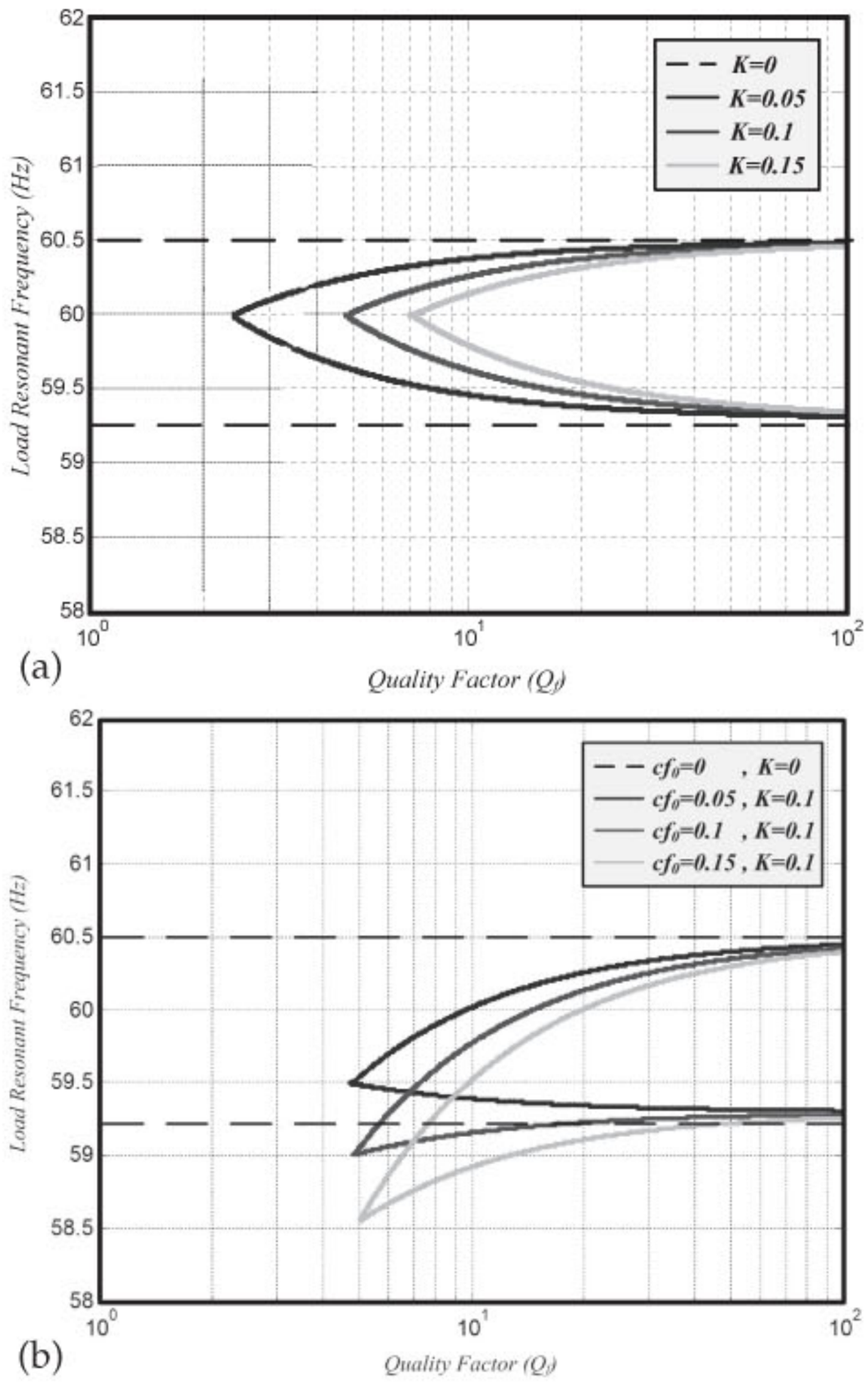

Figure 5: Dependence of NDZ of SFS method on (a) k and (b) Cf_o.

3.2 *Q-f* droop curve

It must be noticed that Q_{ref} is also obtained from *Q-f* droop curve. The DG *Q-f* characteristic is obtained through equation (20).

$$Q_{ref} = K_1 f + K_2 \tag{20}$$

where K_1 and K_2 represent the parameters of the DG *Q-f* characteristic, Q_{ref} is the DG reactive power reference, and f represents the PCC voltage frequency (Zeineldin, 2009) as shown in figure 6. From Zeineldin (2009), it can be seen that the values of the parameters K_1 and K_2 must be chosen such that the DG *Q-f* slope is higher in magnitude than the slope of all possible load curves within the 59.3 and 60.5 Hz window.

Q-f droop curve forces the DG to lose its stable operation once an islanding condition occurs. Although, this method take a lot of time to detect islanding for loads with high quality factor.

3.3 Reactive power deviation

As can be seen in figure 7, Q_{df} is obtained through equation (21), where f_g is the grid frequency, f is the PCC voltage frequency, and K_f is the feedback gain.

$$Q_{df} = K_f(f_g - f) \tag{21}$$

When DG is connected to the grid, system frequency is stable around 60 Hz, which keeps Q_{df} as a small deviation and the system's normal operation is unaffected. While after islanding, the island system frequency depends on the output reactive power and the frequency characteristic of local load. Therefore, the variation of Q_{df} breaks the balance between DG system and local load, and forces the frequency to shift continuously until the islanding is detected (Salman et al, 2011).

3.4 Passive technique

One of the commonly used passive IDM is OFP/UFP and OVP/UVP (Zeineldin & Kirtley, 2009a; 2009b).

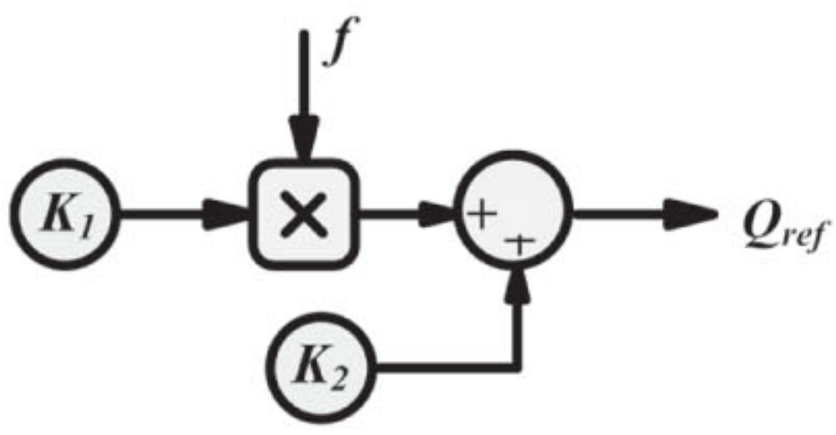

Figure 6: *Q-f* characteristic.

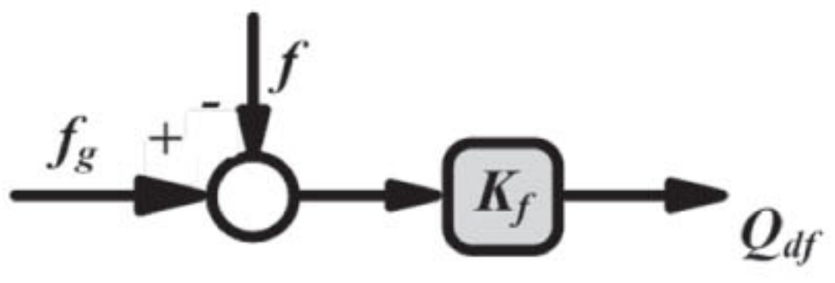

Figure 7: Reactive power deviation.

The OFP/UFP method uses frequency thresholds that are usually set as 59.3 and 60.5 Hz while the OVP/UVP method uses voltage thresholds that are set at 88% and 110% of the nominal voltage value (Zeineldin & Kirtley, 2009a). Upper and lower thresholds are provided to avoid unwilled tripping of the DG due to other system disturbances (Zeineldin & Kirtley, 2009a). Unfortunately, for loads that closely match the DG capacity, the amount of frequency or voltage deviation will not be enough to trigger the IDM (Zeineldin & Kirtley, 2009b). Thus, passive IDMs suffer from large NDZs.

4 NON-DETECTION ZONE OF THE PROPOSED METHOD

The NDZ of the proposed IDM in the Q_f versus f_o space is derived using the phase criteria ($\theta_{load} = \theta_{inv}$):

$$-\tan^{-1}\left[Q_f\left(\frac{f_o}{f_{is}} - \frac{f_{is}}{f_o}\right)\right] = \frac{\pi}{2}\left[Cf_o + k(f_{is} - f_g)\right] + \tan^{-1}(k_1 f_{is} + k_2) \tag{22}$$

Thus:

$$f_o^2 + \frac{f_{is}\tan\left\{\frac{\pi}{2}\left[Cf_o + k(f_{is} - f_g)\right] + k_1 f_{is} + k_2\right\}}{Q_f} f_o - f_{is}^2 = 0 \tag{23}$$

To calculate the NDZ of the proposed IDM, in equation (23) the islanding frequency is first adjusted to a threshold frequency (f_{min} = 59.3 Hz or f_{max} = 60.5 Hz). Then the value of Q_f is varied and finally a calculation is made of the resonant frequency of the load at the threshold of the NDZ. Figure 8 shows the NDZ of proposed method for different values of k, Cf_o, k_1 and k_2 for a normal frequency range of $59.3 < f < 60.5$ Hz. Loads with values of Q_f and f_o lying between the curves calculated with $f_{is} = f_{min}$ and $f_{is} = f_{max}$ are in the NDZ of a given IDM. There one sees that the NDZ

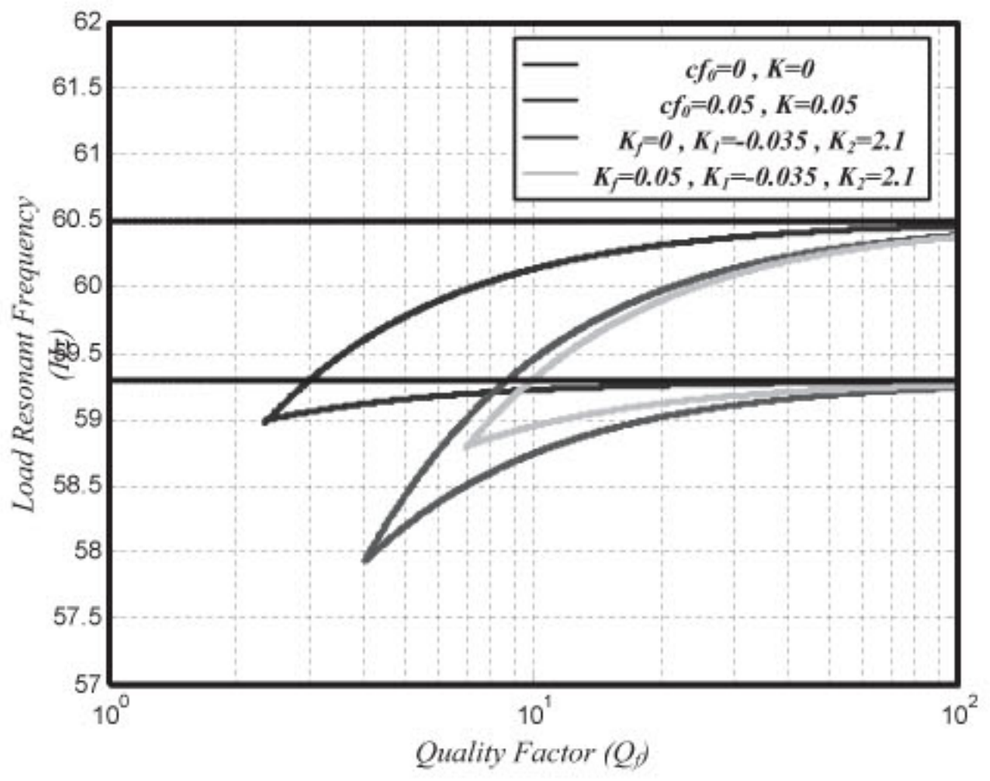

Figure 8: NDZ of proposed islanding detection method.

is null for loads with $Q_f < 3$ when $Cf_o = 0.05$, $k = 0.05$, $k_1 = -0.035$ and $k_2 = 2.1$. In addition, as k_f increases, the load quality factor for which islanding occurs also increases. According to figure 8, it is conspicuous that when $Cf_o = 0.05$, $k = 0.05$, $k_1 = -0.035$, $k_2 = 2.1$ and $k_f = 0.05$, the NDZ is null for loads with $Q_f < 6$. The proposed method is capable of to detect islanding for load with high quality factor. Actually, for $k_1 = 0$ this method becomes the AFD, where for all values of Q_f there will be loads (mostly capacitive) that will lead to islanding. Finally, one sees that the performance of this active IDM, like the others, is equivalent to that of passive UFP/OFP for loads with high Q_f.

5 PERFORMANCE OF THE PROPOSED ISLANDING DETECTION TECHNIQUE

In this section, the system shown in figure 2 is implemented and simulated on MATLAB/Simulink. The inverter, grid, load and DG controller parameters are listed in table 1.

The DG interface control model is implemented and designed to operate as a constant power controlled inverter which is equipped with the proposed method and the SFS, *Q-f* characteristic, RPD parameters are listed in table 3. The IDM is tested for load with a $Q_f = 1.77$. The proposed IDM has been also tested with various loading conditions specified in IEEE 1547 and UL 1741 (Zeineldin et al, 2006).

5.1 UL 1741 testing

Based on the UL 1741 standard, the active load power is adjusted to set the inverter at 25%, 50%, 100% and 125% of the rated output power of the inverter. The reactive power has been adjusted between 95% and 105% of the balanced condition (unity power factor loading) in 1% steps (Zeineldin et al, 2006). The islanding detection scheme is tested based on the procedure offered by Zeineldin et al (2006), but for brevity, samples of the simulation results in this section are provided in table 4. The DG interface is equipped with the proposed method and islanding is occurred at $t = 2$ s.

The first simulation result using the proposed method is shown in figure 9. This figure represents the frequency of voltage at the PCC during an islanding condition, for loads that presented in table 5. It can be seen that, the operation of the DG unit is stable as long as it is connected to the grid. The moment the DG is islanded, the proposed method causes the DG lose

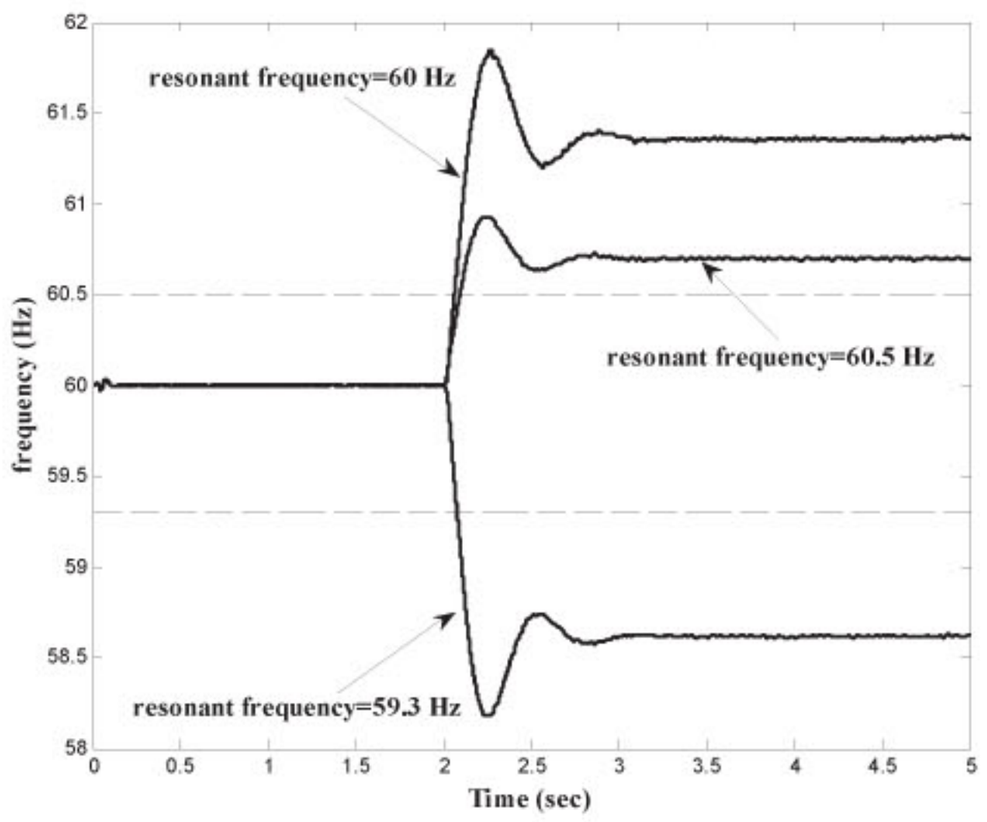

Figure 9: PCC frequency for load with different resonant frequency.

Table 3: Proposed method parameters.

SFS method	$Cf_o = 0.01$	$k = 0.04$
Q-f droop curve	$k_1 = -0.035$	$k_1 = 2.1$
Reactive power deviation	$k_f = 0.015$	

Table 4: Load parameters for UL 1741 testing.

Cases	%*P*	%*Q*	*R* [Ω]	*L* [H]	*C* [μF]	Q_f	f_r
1	100	105	2.304	0.003278	2037	1.81	61.6
2	100	102	2.304	0.003381	2037	1.78	60.6
3	100	101	2.304	0.003419	2037	1.77	60.3
4	100	100	2.304	0.003450	2037	1.77	60.0
5	100	99	2.304	0.003488	2037	1.76	59.7
6	100	98	2.304	0.003519	2037	1.76	59.7
7	100	95	2.304	0.003623	2037	1.73	58.6
8	50	100	4.603	0.003450	2037	3.54	60.0
9	125	100	1.841	0.003450	2037	1.41	60.0

Table 5: Load parameters for different frequency.

R [Ω]	*L* [H]	*C* [μF]	Q_f	f_r
2.304	0.003536	2037	1.74	59.3
2.304	0.003450	2037	1.77	60.0
2.304	0.003397	2037	1.78	60.5

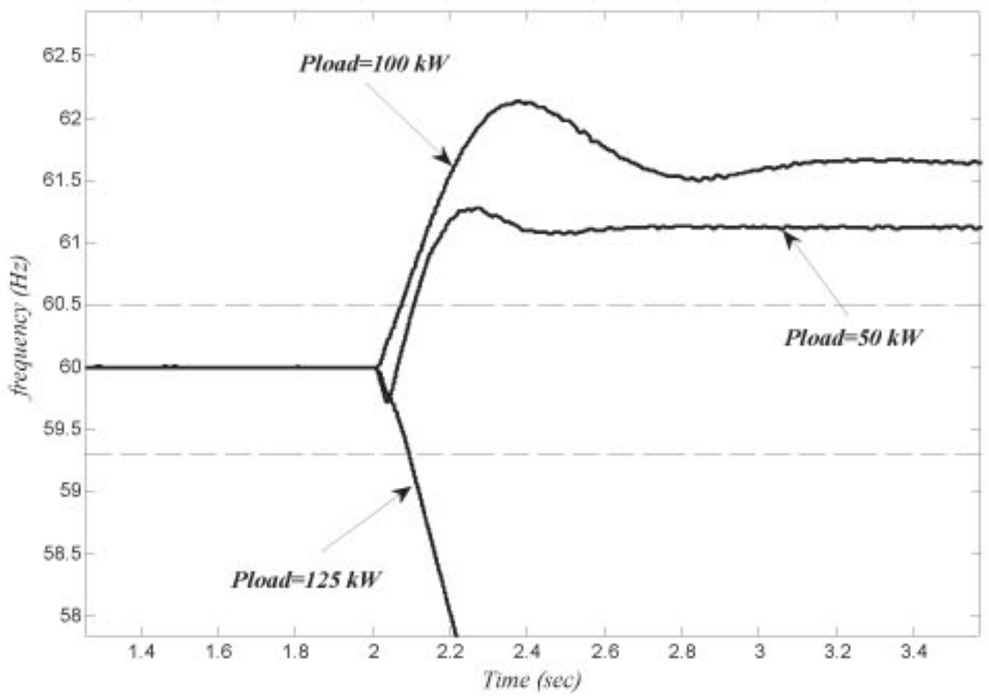

Figure 10: PCC frequency with the proposed method for different active power.

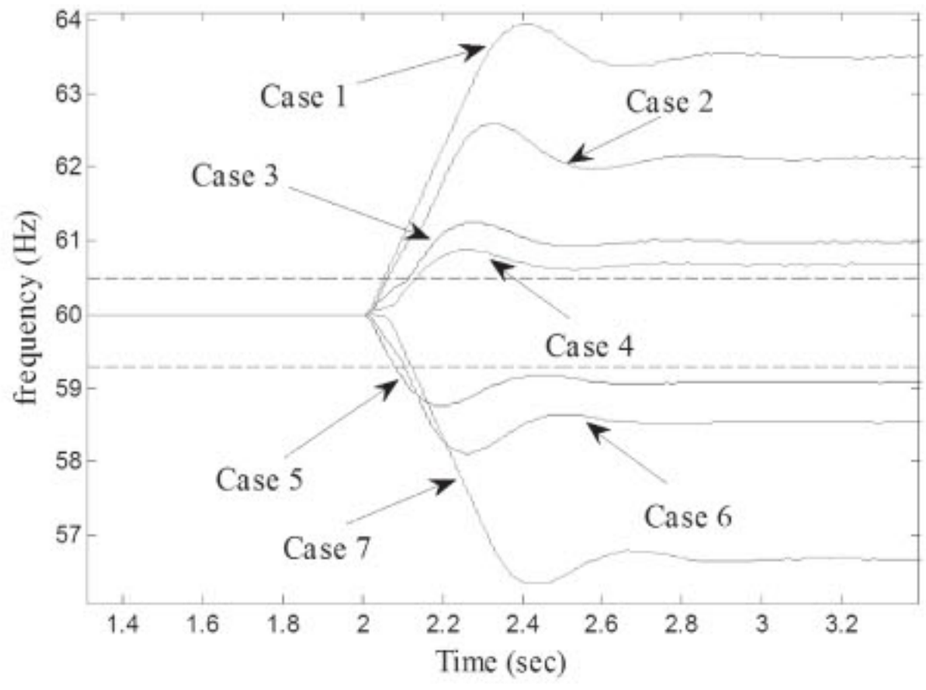

Figure 11: PCC frequency with the proposed method for three cases.

its stable operation, and the PCC frequency deviate and go beyond the over/under frequency (OUF) threshold value for the presented cases.

Figure 10 shows the frequency of voltage at the PCC during an islanding condition, with the proposed technique, when the active load power is adjusted to set the inverter at 50%, 100% and 125% of its rated output. Also, the reactive power is adjusted at 100% of the balanced condition. It can be seen from figure 10, the frequency measured at the PCC exceeds the OUF thresholds in less than 100 ms (after the event of islanding).

In the next sample of results, the frequency at the PCC during an islanding condition, for the following cases, is shown in figure 11 (Zeineldin, 2009):

- Case 1. Load is adjusted to operate the inverter at 100% of its rated active power output and 105% reactive power balanced.
- Case 2. Load is adjusted to operate the inverter at 100% of its rated active power output and 102% reactive power balanced.
- Case 3. Load is adjusted to operate the inverter at 100% of its rated active power output and 101% reactive power balanced.
- Case 4. Load is adjusted to operate the inverter at 100% of its rated active power output and 100% reactive power balanced.
- Case 5. Load is adjusted to operate the inverter at 100% of its rated active power output and 99% reactive power balanced.
- Case 6. Load is adjusted to operate the inverter at 100% of its rated active power output and 98% reactive power balance.
- Case 7. Load is adjusted to operate the inverter at 100% of its rated active power output and 95% reactive power balanced.

Similarly, once an islanding condition occurs at $t = 2$ s, the DG loses its stable operation, and the frequency deviates and exceeds the OUF threshold values. For the cases presented in figure 11, the frequency exceeds the OUF threshold in less than 115 ms.

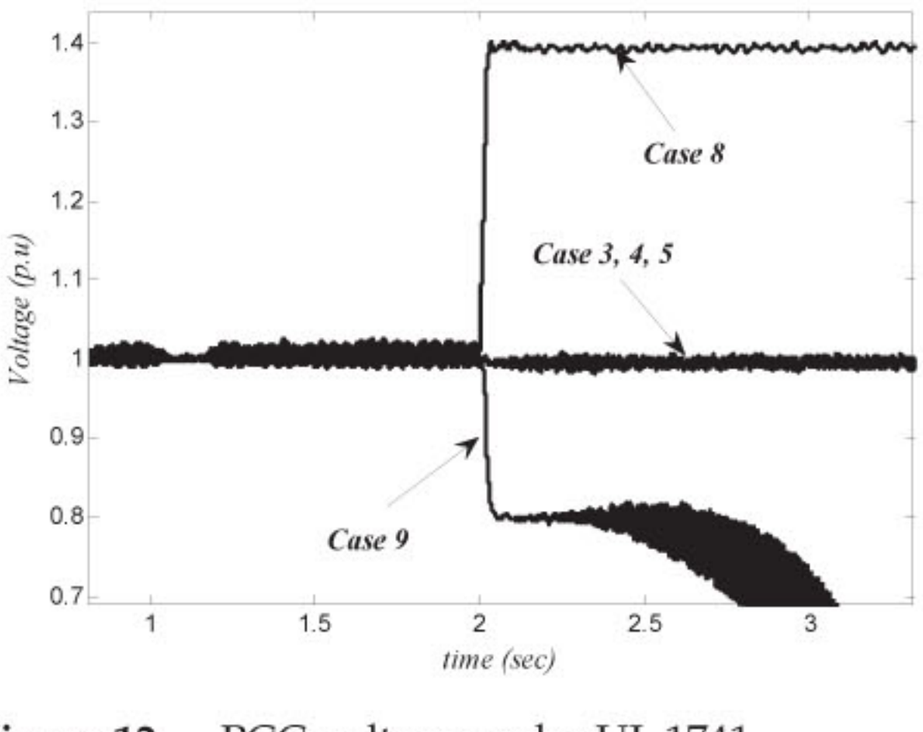

Figure 12: PCC voltage under UL 1741 testing condition.

Voltages of the PCC during an islanding condition for the UL1741 testing condition, with the proposed method are shown in figure 12. According to this figure, it is clear that the proposed method for cases that load active power is adjusted to set the inverter at 100% of its rated output, is not able to deviate the voltage at the PCC beyond the voltage relays threshold values such as UVP/OVP (cases 3, 4 and 5 in table 4). For cases that the load active power is adjusted to set the inverter at 50% and 125% of load output power (cases 8 and 9 in table 4), the proposed method causes the DG lose its stable operation, and the voltage at the PCC deviate and go beyond the UVP/OVP threshold values and islanding can be detected.

Figure 13 shows the frequency of the voltage at the PCC during an islanding condition for the UL 1741 testing condition while the DG interface controller is equipped with the SFS IDM. According to this figure, it can be seen that the constant power controlled inverter equipped with the SFS IDM is not able to detect the islanding phenomena for UL 1741 testing conditions.

5.2 Effect of load switching

The proposed IDM is tested for load switching in the grid-connected operation mode. Similar to the

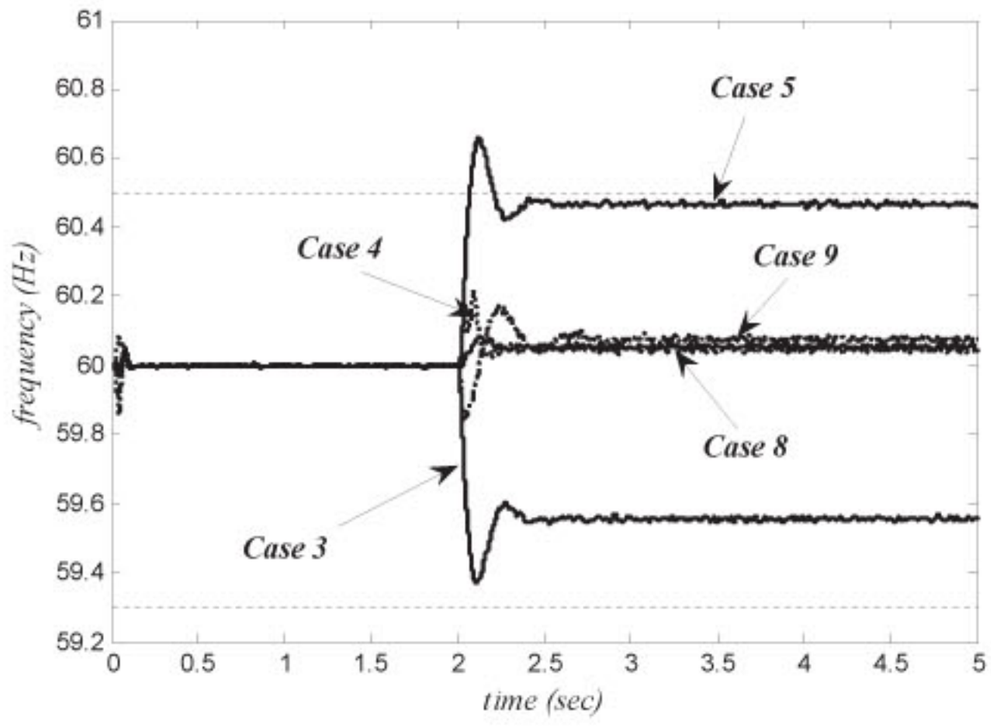

Figure 13: PCC frequency for UL1741 testing condition with the SFS method.

old load, which has been presented in figure 2, the new load is switched at t = 2 s and disconnected at t = 3 s, which is shown in figure 14. Three cases have been simulated in this test. In all cases, the load real power is equal to 100 kVA but the power factor is 0.8 lead, 1.0 and 0.8 lag. The simulation results that include the PCC voltage, frequency, active and reactive powers for three different loading conditions are shown in figures 15 and 16. The voltage and frequency variations can be seen when the load is switched on and off. For simulated cases, the voltage and frequency variations are within the standard values. It is clear that the proposed method does not interfere with the power system operation during normal conditions.

5.3 Influence of load quality factor

The IEEE Standard 929 proposes the use of $Q_f \leq 2.5$ as test condition. However, IEEE 1547.1 suggests testing islanding with loads having a quality factor of 1 (Woyte et al, 2003). The UL 1741 test specifies that an IDM must succeed in detecting the islanding phenomenon within 2 s for R-L-C loads with $Q_f \leq 1.8$ (Zeineldin, 2009). For the system shown in figure 2, Q_f has changed in the range of 0.5 to 8.1 by adjusting the load inductance and capacitance according to table 6. The real load power is adjusted to put inverter at 100% of the inverter's rated output for all cases. The load inductance and capacitance were differed such that the load reactive power was set at 100% of the balanced condition. The PCC frequency measured for different values of Q_f are shown in figure 17. For the range of Q_f under study, the frequency has exceeded the OUF thresholds in less than 100 ms for Q_f = 0.5 and 115 ms for Q_f = 8.1. Also, proposed method can be detect islanding in less than 75 ms for Q_f = 1.77 and 135 ms for Q_f = 6.38.

Figure 18 shows the frequency of the voltage at the PCC during an islanding condition for loads with high quality factors while the DG interface controller is equipped with the SFS IDM. According to this figure, it can be seen that constant power controlled inverter

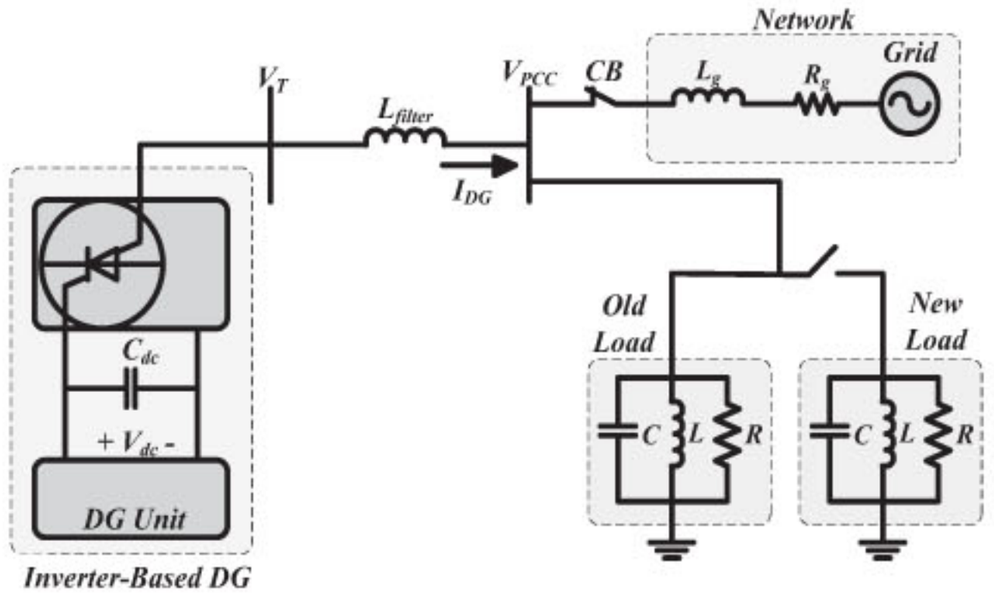

Figure 14: System under study for load switching.

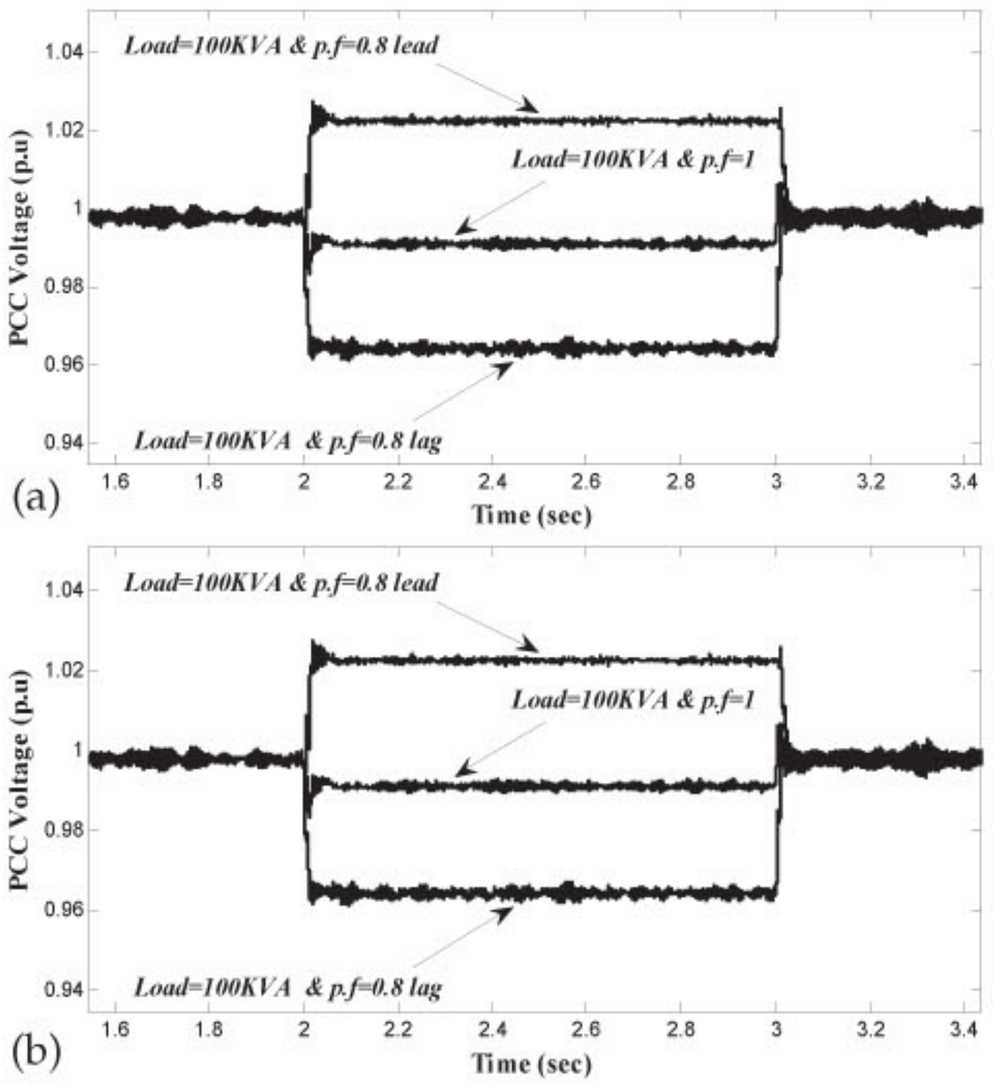

Figure 15: PCC (a) voltage and (b) frequency during a load switching event.

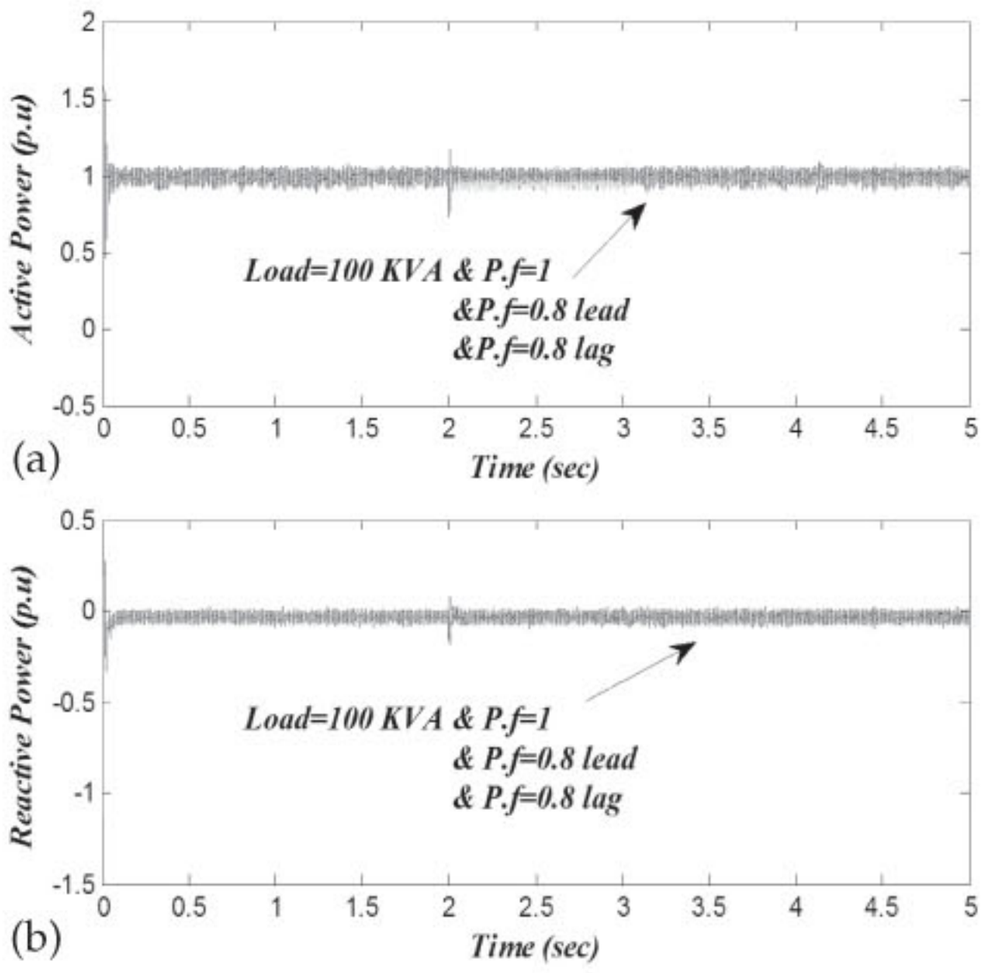

Figure 16: (a) Active and (b) reactive power of the PCC during a load switching event.

Table 6: Load parameters for different values of Q_f.

R [Ω]	L [H]	C [μF]	Q_f	f_r
2.304	0.012200	575.4	0.50	60.07
2.304	0.006100	1150.0	1.00	60.10
2.304	0.003450	2037.0	1.77	60.00
2.304	0.002030	3452.0	3.00	60.12
2.304	0.001450	4850.0	4.21	60.00
2.304	0.000957	7350.0	6.38	60.00
2.304	0.000754	9330.0	8.10	60.00

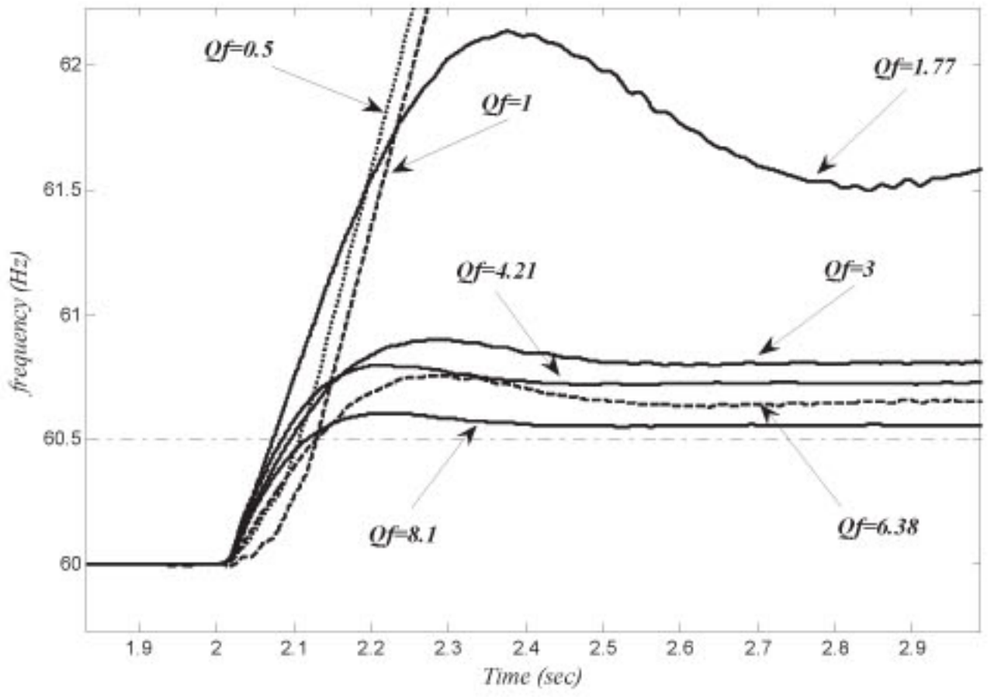

Figure 17: PCC frequency with the proposed IDM for different values of Q_f.

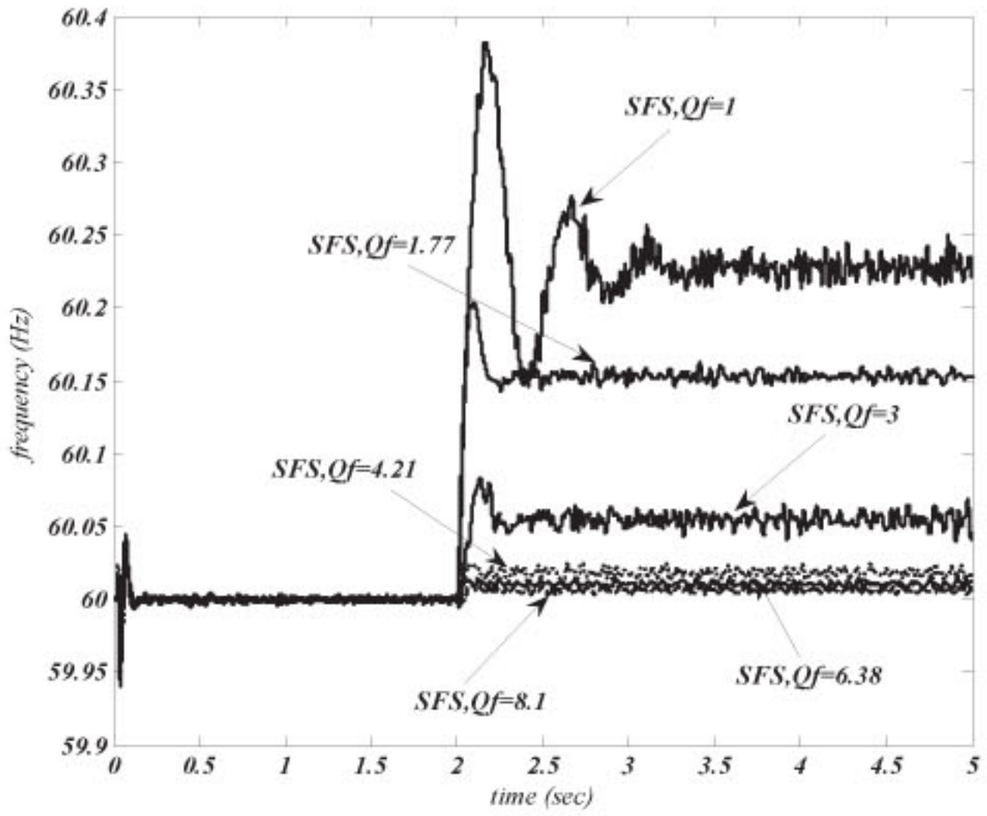

Figure 18: PCC frequency with the SFS IDM for different value of Q_f.

equipped with the SFS IDM is not able to detect the islanding phenomena for loads with high quality factors that are shown in table 6. In contrast to, the proposed method could able to detect the islanding situation easily for loads with high quality factors.

5.4 Multiple-DG operation mode

The proposed IDM was further tested in a system with multiple DGs. Two identical DGs, each with a

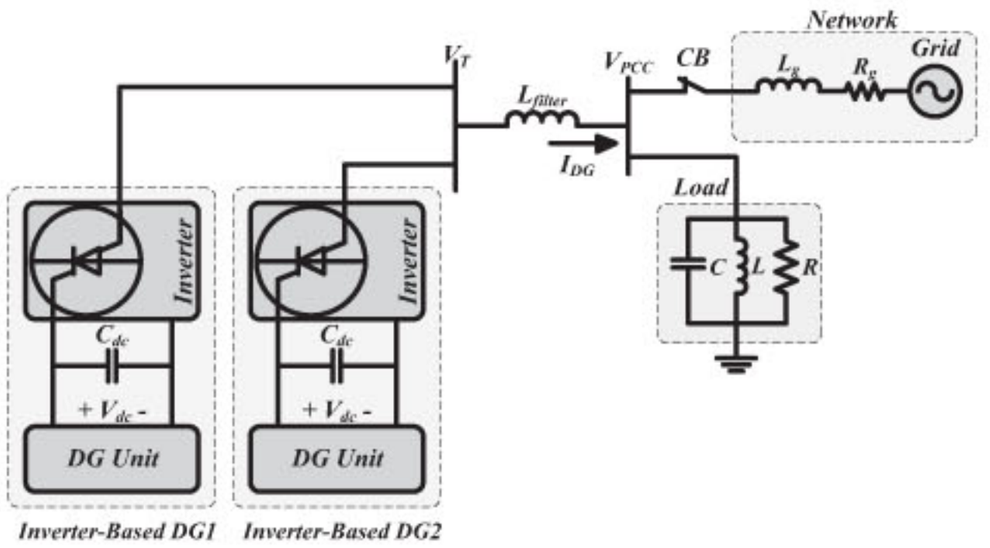

Figure 19: System under study for the multiple-DG operation mode.

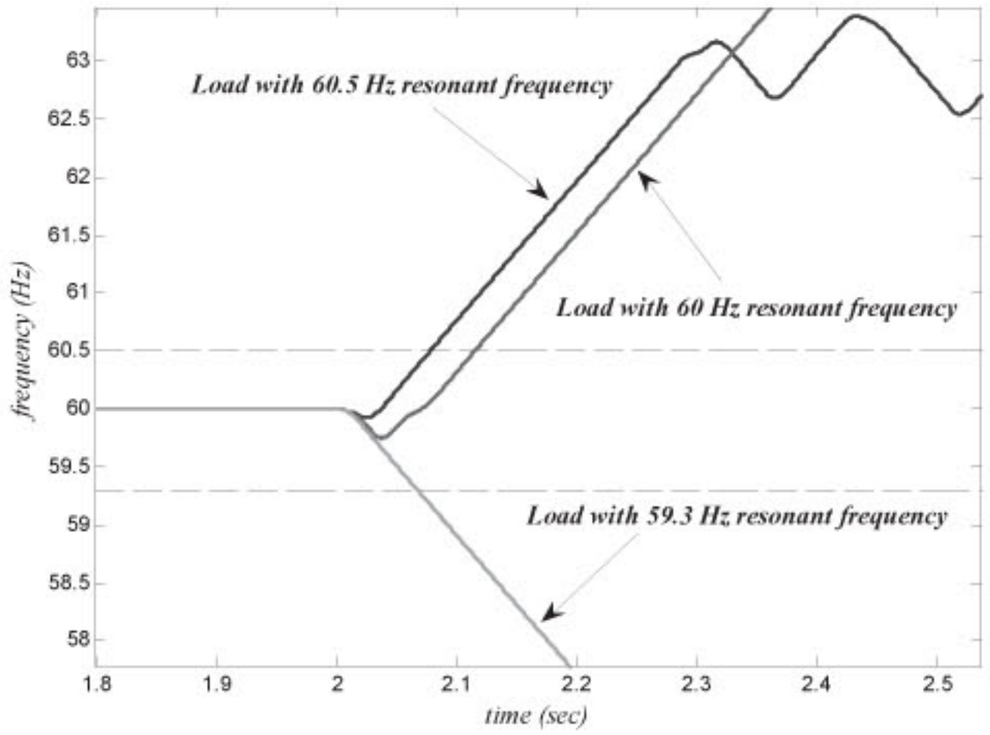

Figure 20: PCC frequency for the multiple-DG operation mode.

100 kW rated output power, are connected at the PCC. Figure 19 illustrates the operation of two DGs grid-connected inverters. Each DG interface is equipped with the proposed method shown in figure 3. The real load power was adjusted to place the inverter at 100% (200 kW) of the inverter's rated output power for all cases. Islanding has been simulated at $t = 2$ s and the load has Q_f of 0.885. The simulation result has been presented in figure 20. It can be seen that DG loses its stable operation mode, and an islanding condition can be detected by using OUF/OUV methods in 70, 130 and 170 ms for load with resonant frequency 59.3, 60.0 and 60.5 Hz, respectively.

6 CONCLUSION

In this paper, a new hybrid IDM for inverter based DGs is proposed. This method is relies on equipping the DG interface with SFS, *Q-f* droop curve and RPD as active methods. The proposed method is chosen such that the DG maintains its stable operation while grid-connected and loses its stability once an islanding condition occurs. With a DG equipped with the proposed method, the OFP/UFP is adequate for efficiently and precisely to detect islanding. By implementing the proposed method, the OFP/UFP method will have a negligible NDZ.

The proposed hybrid islanding detection technique is studied for the inverter-based DG unit under the

IEEE 1547 and UL 1741 test conditions, multiple-DG operation mode, load switching conditions and various load quality factor. Based on simulation results, it is found that the proposed method for cases where the DG and load closely match in terms of active and reactive powers and multiple DG operation modes is capable of detecting an islanding situation within the minimum standard time. For loads with high quality factor and different loading conditions also the proposed technique is capable of detecting islanding within the standard allowable detection times. In addition, a DG equipped with the proposed technique will be capable of maintaining stable operation when tested under load switching condition.

REFERENCES

Chang, W. Y. 2013, "A Passive Islanding Detection Method for Grid-Connected Renewable Generation System", *Applied Mechanics and Materials*, Vol. 284-287, pp. 1182-1186.

De Mango, F., Liserre, M. & Aquila, A. D. 2006, "Overview of Anti Islanding Algorithms for PV Systems. Part II: Active Methods", *12th International Power Electronics and Motion Control Conference (EPE-PEMC 2006)*, 30 August to 1 September, pp. 1884-1889.

Freitas, W., Xu, W., Affonso, C. M. & Huang, Z. 2005, "Comparative analysis between ROCOF and vector surge relays for distributed generation applications", *IEEE Transactions on Power Delivery*, Vol. 20, No. 2, April, pp. 1315-1324.

Huang, S.-J. & Pai, F.-S. 2000, "A new approach to Islanding detection of dispersed generators with self-commutated static power converters", *IEEE Transactions on Power Delivery*, Vol. 15, No. 2, April, pp. 500-507.

IEEE, 2003, *IEEE 1547-2003 Standard for Interconnecting Distributed Resources Electric Power Systems*, July.

Kamyab, E. & Sadeh, J. 2013, "An Islanding Detection Method for Photovoltaic Distributed Generation Based On Voltage Drifting", *IET Generation, Transmission & Distribution*, Vol. 7, No. 6, June, pp. 584-592.

Kim, J. E. & Hwang, J. S. 2000, "Islanding detection method of distributed generation units connected to power distribution system", *International Conference on Power System Technology (PowerCon 2000)*, 4-7 December, Vol. 2, pp. 643-647.

Liu, B. & Thomas, D. 2011, "New Islanding Detection Method for DFIG Wind Turbines", *4th International Conference on Electric Utility Deregulation and Restructuring and Power Technologies (DRPT)*, 6-9 July, Weihai, Shandong, pp. 213-217.

Lopes, L. A. C. & Sun, H. 2006, "Performance assessment of active frequency drifting Islanding detection methods", *IEEE Transactions on Energy Conversion*, Vol. 21, No. 1, March, pp. 171-180.

Massoud, A. M., Ahmed, K. H., Finney, S. J. & Williams, B. W. 2009, "Harmonic distortion-based Island detection technique for inverter-based distributed generation", *IET Renewable Power Generation*, Vol. 3, No. 4, December, pp. 493-507.

Ropp, M. & Bower, W. 2002, *Evaluation of islanding detection methods for photovoltaic utility interactive power systems*, International Energy Agency, Implementing Agreement Photovoltaic Power Systems, Task V, Report IEA-PVPS T5-09: 2002, March, http://apache.solarch.ch/pdfinter/solar/pdf/pvpstask509.pdf.

Salman, S. K., King, D. J. & Weller, G. 2011, "New loss of mains detection algorithm for embedded generation using rate of change of voltage and changes in power factors", *Seventh International Conference on Developments in Power System Protection*, 9-12 April, Amsterdam, pp. 82-85.

Singam, B. & Huil, Y. 2006, "Assessing SMS and PJD Schemes of Anti Islanding with Varying Quality Factor", *IEEE International Power and Energy Conference (PECon '06)*, 28-29 November, pp. 196-201.

Underwriters Laboratories, Inc., 2001, *Static Inverter and Charge Controllers for Use in Photovoltaic Systems Standard UL*, Northbrook, IL.

Vahedi, H. & Karrari, M. 2013, "Adaptive Fuzzy Sandia Frequency-Shift Method for Islanding Protection of Inverter-Based Distributed Generation", *IEEE Transactions on Power Delivery*, Vol. 28, No. 1, January, pp. 84-92.

Vahedi, H., Noroozian, R., Jalilvand, A. & Gharehpetian, G. B. 2011, "A new method for islanding detection of inverter-based distributed generation using DC-link voltage control", *IEEE Transactions on Power Delivery*, Vol. 26, No. 2, April, pp. 1176-1186.

Wang, X., Freitas, W., Xu, W. & Dinavahi, V. 2007, "Impact of DG interface controls on the Sandia frequency shift anti-islanding method", *IEEE Transactions on Energy Conversion*, Vol. 22, No. 3, September, pp. 792-794.

Woyte, A., Belmans, R. & Nijs, J. 2003, "Testing the islanding protection function of photovoltaic inverters", *IEEE Transactions on Energy Conversion*, Vol. 18, No. 1, March, pp. 157-162.

Zeineldin, H. H. 2009, "A (Q-f) droop curve for facilitating islanding detection of inverter-based distributed generation", *IEEE Transactions on Power Electronics*, Vol. 24, No. 3, March, pp. 665-673.

Zeineldin, H. H. & Kennedy, S. 2009a, "Sandia Frequency-Shift Parameter Selection to Eliminate Non detection Zones", *IEEE Transactions on Power Delivery*, Vol. 24, No. 1, January, pp. 486-488.

Zeineldin, H. H. & Kennedy, S. 2009b, "Instability Criterion to Eliminate the Non-detection Zone of the Sandia Frequency Shift Method", *IEEE/PES Power Systems Conference and Exposition (PSCE '09)*, 15-18 March, Seattle, WA, pp. 1-5.

Zeineldin, H. H. & Kirtley, J. L. 2009a, "Performance of the OVP/UVP and OFP/UFP Method With Voltage and Frequency Dependent Loads", *IEEE Transactions on Power Delivery*, Vol. 24, No. 2, April, pp. 772-778.

Zeineldin, H. H. & Kirtley, J. L. 2009b, "A simple technique for islanding detection with negligible non-detection zone", *IEEE Transactions on Power Delivery*, Vol. 24, No. 2, April, pp. 779-786.

Zeineldin, H. H. & Salama, M. M. A. 2011, "Impact of load frequency dependence on the NDZ and performance of the SFS islanding detection method", *IEEE Transactions on Industrial Electronics*, Vol. 58, No. 1, January, pp. 139-146.

Zeineldin, H. H., EI-Saadany, E. F. & Salama, M. M. A. 2006, "Impact of DG interface control on islanding detection and non-detection zones", *IEEE Transactions on Power Delivery*, Vol. 21, No. 3, July, pp. 1515-1523.

Zhou, X., Wu, J. & Ma, Y. 2013, "A Review of Islanding Detection Method of Grid-connected PV Power System", *Advanced Materials Research*, Vol. 614-615, pp. 815-818.